PERGAMON

Chemical Engineering Science 56 (2001) 3737–3750

Chemical Engineering Science

www.elsevier.nl/locate/ces

Scaling relationships for rotating drums

Y. L. Ding[a,*], R. N. Forster[b], J. P. K. Seville[a], D. J. Parker[b]

[a] School of Chemical Engineering, University of Birmingham, Edgbaston, Birmingham B15 2TT, UK
[b] School of Physics and Astronomy, University of Birmingham, Edgbaston, Birmingham B15 2TT, UK

Received 10 May 2000; received in revised form 30 January 2001; accepted 1 March 2001

Abstract

Rotating drums are extensively used in the chemical and process industries as kilns, mixers, dryers and reactors. Despite challenges from the development of newer and more specialised technologies such as fluidised beds, rotating drums continue to find applications. This is mainly due to their ability to handle varying feed stocks, in particular granular materials with broad particle size distribution and significant difference in physical properties. However, the scale-up methodology for such devices is still largely empirical and no general and systematic method has been established. This work is therefore devoted to the development of a set of scaling relationships which can be used to properly design rotating drums. The scaling relationships are obtained by non-dimensionalising the differential equations governing the behaviour of solids motion in rotating drums. The derived dimensionless groups include Froude number, pseudo-Reynolds number, pseudo-Euler number, drum geometric ratios, drum inclination, drum fill percentage, size distribution of particles, and physical properties of the particles and drum wall such as restitution coefficient and elasticity modulus. At relatively low pseudo-Reynolds numbers, the effect of velocity fluctuation and hence the granular temperature can be neglected, the granular flows are thus in the quasi-static regime. At relatively low pseudo-Euler numbers, the effect of the frictional contribution to the total stress tensor is negligible and the flow is in the rapid granular flow regime. The upper limit of the quasi-static regime is evaluated and the adequacy of the application of granular flow kinetic theory to rotating drums is discussed. It is shown that granular flows in large drums operated at low to medium rotational speeds are often in the quasi-static regime, whereas those in small drums operated at medium rotational speeds may be in the transition flow regime. Preliminary experiments have been carried out with the aim of reducing the total number of controlling dimensionless groups. The dimensionless groups investigated include the drum length-to-diameter ratio, rotational Froude number, fill percentage, particle-to-drum diameter ratio, particle restitution coefficient, and the relative drum wall roughness. It is shown that the Froude number, particle-to-drum diameter ratio, drum fill percentage, and particle restitution coefficient can be combined to give a single dimensionless parameter if drums are operated in a rolling mode and the Froude number is greater than 0.003.

Keywords: Rotating drum; Scaling relationships; Solids mixing; Granular flow; Rolling mode

1. Introduction

Granular material processing such as calcination of limestone, reduction of iron oxide, clinkering of cementitious materials, production of pigment, decoating of aluminium scrap, cereal drying and even waste incineration often involves the utilisation of rotating drums. Despite considerable effort by previous workers, scale-up methodology for such devices is still largely empirical and no general and systematic method has been established.

One of the most difficult issues in the establishment of the scaling relationships for rotating drums lies in the complexity of the modes of solids motion. Six modes of bed movement have been identified (Rutgers, 1965; Henein, Brimacombe, & Watkinson, 1983). With increasing rotational speed, these are slipping, slumping, rolling, cascading, cataracting, and centrifuging modes. Although the Froude number and drum fill percentage have been proposed to describe the transitions between these modes (Henein et al., 1983), it is expected that other factors such as the rheological properties of the particles and the physical properties of the drum wall will also exert some influence. In addition, for drums with very long aspect ratios (length/diameter), different modes of solids

* Corresponding author. Tel.: +44-0121-414-5303; fax: +44-0121-414-5324.
E-mail address: y.ding@bham.ac.uk (Y. L. Ding).

0009-2509/01/$ - see front matter
PII: S0009-2509(01)00092-6

motion may occur simultaneously within the drum. The gas phase may also have a substantial influence on the behaviour of small particles at high rotational speeds. All these add intricacies to the derivation of the scale-up relationships.

Although six modes of solids motion have been observed, industrial-scale drums are often operated in the rolling or slumping mode. This paper is therefore focused on rotating drums operated in or not far from the rolling mode. The scale-up relationships are derived from fundamental equations that govern solids motion in rotating drums. In Section 2, a brief summary of the governing equations and relevant constitutive relationships is presented and discussed. These equations are then non-dimensionalised in Section 3 to obtain dimensionless groups. Discussion of these dimensionless numbers is made in Section 4 to obtain the controlling parameters. In Section 5, preliminary experimental results are presented and future work is discussed. Previous work relevant to the scale-up of rotating drums is also presented where appropriate.

2. Governing equations for solids motion in rotating drums

2.1. Continuum model and particulate theory

Broadly speaking, two methods can be used to describe solids motion in rotating drums, i.e. continuum (Eulerian) and the particulate (Lagrangian) approaches. The Lagrangian method employs Newton's second law in the description of particle motion; see for example Walton and Braun (1993), Yamane (1997), and Cleary, Metcalfe, and Liffman (1998). The Eulerian method assumes that the properties of the granular material are continuous functions of position (Cowin, 1974; Haff, 1983; Lun, Savage, Jeffery, & Chepurniy, 1984; Johnson & Jackson, 1987; Savage & Hutter, 1989). In this work, the Eulerian approach will be used in the derivation of the scaling relationships, which in theory should give results which are equivalent to the Lagrangian method.

2.2. Governing equations based on the Eulerian approach

The equations governing solids motion in rotating drums consist of conservation of mass and momentum. As the focus of this work is on rotating drums operated in or not far from the rolling mode, the effect of the fluid phase is neglected. For simplicity, granular material with uniform particle size is considered. The consequences of this simplification will be taken up in a later section of this paper. The mass and momentum balances are given as:

$$\frac{\partial \rho}{\partial t} + \nabla \cdot (\rho \vec{u}) = 0, \tag{1}$$

$$\frac{\partial \vec{u}}{\partial t} + \vec{u} \cdot \nabla \vec{u} = \vec{F} - \frac{1}{\rho} \nabla \cdot (\vec{P}_R + \vec{P}_S), \tag{2}$$

where $\rho = \rho_p v$ is the bulk density of the granular material, ρ_p is the particle material density, v is the solid volumetric fraction, $\vec{u}$ is the velocity vector, $\vec{F}$ is the body force vector, $\vec{P}_R$ is the sum of kinetic (streaming) and collisional contributions to the total stress tensor, and $\vec{P}_S$ is the frictional contribution to the total stress tensor. The streaming or kinetic part of $\vec{P}_R$ accounts for the transport of particle properties as the particles move freely across void space in the flow. The collisional part of $\vec{P}_R$ accounts for transfer of momentum during collisional interaction between particles. Eq. (2) assumes that the total stress in the granular continuum is the sum of the frictional contribution, and the streaming and collisional contributions. These contributions are calculated independently from constitutive expressions derived for the limits of purely collisional and streaming contributions, and purely frictional contribution, respectively. This treatment has not been fully verified so far. However, this should not affect the results of this work, as the formulation of terms in the stress tensor does not affect the dimensionless groups obtained.

According to the dense-gas kinetic theory, the individual particle motions are composed of a mean component and a random component, and $\vec{P}_R$ can be related to the so-called granular temperature (defined as the average of the sum of the squares of the three random components of particle velocity). Due to the introduction of granular temperature, a pseudo-thermal energy equation is required to close the problem:

$$\frac{3}{2}\rho \left(\frac{\partial T}{\partial t} + \vec{u} \cdot \nabla T \right) = -\vec{P}_R \colon \nabla \vec{u} - \nabla \cdot \Gamma - \gamma, \tag{3}$$

where T is granular temperature, Γ is pseudo-thermal energy flux due to conduction, and γ is specific pseudo-thermal energy dissipation due to inelastic particle collisions. Eq. (3) assumes that the frictional contribution to the total stress does not affect the balance of the pseudo-thermal energy.

The constitutive relations for $\vec{P}_R$, γ, Γ, and $\vec{P}_S$ are, respectively, given as (Lun et al., 1984; Johnson & Jackson, 1987):

$$\vec{P}_R = [\rho_p g_1(v, e_p) T - \rho_p d_p \frac{8}{3\sqrt{\pi}} \eta v^2 g_0 T^{1/2} \nabla \cdot \vec{u}] I$$

$$-2[\rho_p d_p g_2(v, e_p) T^{1/2}] S, \tag{4}$$

$$\Gamma = -\rho_p d_p [g_3(v, e_p) T^{1/2} \nabla T + g_4(v, e_p) T^{3/2} \nabla v], \tag{5}$$

$$\gamma = \frac{\rho_p}{d_p} g_5(v, e_p) T^{3/2}, \tag{6}$$

$$\vec{P}_S = N_S \vec{n}_u + S_S \vec{t}_u, \tag{7}$$

where e_p is particle restitution coefficient, d_p is particle diameter, $\eta = (1+e_p)/2$, I is the identity matrix, S is the deviatoric part of the rate of deformation tensor given by:

$$S = \tfrac{1}{2}(u_{n,p} + u_{p,n}) - \tfrac{1}{3} u_{ll} \delta_{np} \ (l, n, p = x, y, z, \ \delta_{np} = 1 \text{ for } n = p, \ \delta_{np} = 0 \text{ for } n \neq p), \tag{8}$$

g_i ($i = 0$–5) are functions of v and e_p and are respectively given as:

$$g_0 = \left(1 - \frac{v}{v_m}\right)^{-2.5 v_m}, \tag{9}$$

$$g_1(v, e_p) = v + 4\eta v^2 g_0, \tag{10}$$

$$g_2(v, e_p) = \frac{5\sqrt{\pi}}{96} \left[\frac{1}{\eta(2-\eta) g_0} + \frac{8}{5} \frac{3\eta - 1}{2 - \eta} v + \frac{64}{25} \eta \left(\frac{3\eta - 2}{2 - \eta} + \frac{12}{\pi} \right) v^2 g_0 \right], \tag{11}$$

$$g_3(v, e_p) = \frac{25\sqrt{\pi}}{16\eta(41 - 33\eta)} \left\{ \frac{1}{g_0} + \frac{12}{5} \eta [1 + \eta(4\eta - 3)] v + \frac{16}{25} \eta^2 [9\eta(4\eta - 3) + \frac{4}{\pi}(41 - 33\eta)] v^2 g_0 \right\}, \tag{12}$$

$$g_4(v, e_p) = \frac{15\sqrt{\pi}}{4} \frac{(2\eta - 1)(\eta - 1)}{41 - 33\eta} \left(\frac{1}{v g_0} + \frac{12}{5} \eta \right) \frac{\mathrm{d}}{\mathrm{d}v}(v^2 g_0), \tag{13}$$

$$g_5(v, e_p) = \frac{48}{\sqrt{\pi}} \eta (1 - \eta) v^2 g_0, \tag{14}$$

where v_m is the maximum shearable solid fraction for the particle assembly. $\vec{n}_u$ and $\vec{t}_u$ in Eq. (7) are unit vectors in the normal and tangential directions, while N_S and S_S denote the frictional contributions to the normal and tangential stresses, respectively. According to Johnson, Nott, and Jackson (1990), N_S and S_S can be given as:

$$S_S = N_S \sin \phi, \tag{15}$$

$$N_S = F_S \frac{(v - v_{\min})^{n_1}}{(v_m - v)^{n_2}} \quad (v > v_{\min}) \quad = 0 \quad (v \leqslant v_{\min}), \tag{16}$$

where ϕ is the frictional angle, F_S, n_1 and n_2 are constants, and $v_{\min}$ corresponds to the value of v when evenly distributed particles no longer touch. Obviously, the frictional contribution to the total stress tensor is rate independent.

The derivation of Eqs. (4)–(6) and (8)–(14) involves the following assumptions: (a) particle interactions are binary and instantaneous; (b) particles are hard spheres with a smooth surface; (c) particles are slightly inelastic and (d) particle motion is chaotic (similar to Boltzmann's *stosszahlansatz*), see for example Lun et al. (1984), Haff (1983), Savage and Hutter (1989) and Campbell (1990). For granular flows with small to moderate particle concentrations, assumptions (a) and (d) have been shown to be approximately applicable (Walton & Braun, 1986; Drake, 1988; Lan & Rosato, 1995). At high solid volumetric concentrations, assumptions (a) and (d) break down. This, however, does not affect this work as the frictional contribution to the total stress dominates in this case. More discussion on this will be given in Section 4. According to computer simulations carried out by Lun et al. (1984) and Walton and Braun (1986), assumption (c) is not very strict as the model for slightly inelastic particles applies approximately to the case of particle restitution coefficients as low as 0.6. Smooth spherical particles can hardly be found in practice. Lun (1991) derived a general set of conservation equations and constitutive integrals for the dynamic properties of the rapid flow of slightly inelastic and slightly rough spherical particles. Apart from the equations introduced earlier, his theory involves two more equations for angular momentum and rotational granular temperature balances and four more constitutive relations. As for non-spherical particles, mathematical treatment will be very complicated and sometimes even impossible. As a consequence, assumption (b) provides a significant simplification to the problem. In order to catch the main features of granular flows consisting of non-spherical and rough particles, particle surface roughness, particle frictional coefficient and particle shape factor are often used to take up the consequence of assumption (b), see Section 4.1.

3. Non-dimensionalisation of the governing equations

The velocity will be non-dimensionalised with respect to the characteristic velocity of the granular material in a drum, U_0, which may be the linear velocity of the drum, or the average radial- or axial-direction velocity:

$$\bar{\vec{u}} = \vec{u}/U_0. \tag{17}$$

Additional dimensionless quantities are:

$$\bar{t} = U_0 t / d_p, \tag{18}$$

$$\bar{\nabla} = d_p \nabla, \tag{19}$$

$$\bar{S} = (d_p/U_0) S, \tag{20}$$

$$\bar{T} = T/T_0, \tag{21}$$

$$\bar{v} = v/v_r, \tag{22}$$

$$\bar{N}_S = N_S/N_0, \tag{23}$$

$$\bar{S}_S = S_S/S_0, \tag{24}$$

$$\bar{g}_0 = g_0(v)/g_r(v_r), \quad \bar{g}_i = g_i(v, e_p)/g_{ir}(v_r, e_p) \quad (i = 1\text{–}5), \tag{25}$$

where $g_r(v_r) = g_0(v_r)$, $g_{ir}(v_r,\ e_p) = g_i(v_r, e_p)$, T_0 is the reference granular temperature, N_0 and S_0 are the reference values for N_s and S_s, respectively, and v_r is the reference solid volumetric fraction.

3.1. Dimensionless continuity equation

Insertion Eqs. (17)–(19) and (22) into Eq. (1) gives the non-dimensional form of the continuity equation:

$$\frac{\partial \bar{v}}{\partial \bar{t}} + \nabla \cdot (\bar{v}\vec{\bar{u}}) = 0. \tag{26}$$

In the derivation of Eq. (26), $\rho = \rho_p v$ has been used.

3.2. Dimensionless momentum equation

Inserting Eqs. (17)–(25) into Eq. (2) and considering Eqs. (4)–(16) yields the following dimensionless momentum equation:

$$\begin{aligned}\frac{\partial \vec{\bar{u}}}{\partial \bar{t}} + \vec{\bar{u}} \cdot \bar{\nabla}\vec{\bar{u}} = {} & \frac{g d_p}{U_0^2}\vec{l} - \left[\frac{g_{1r}(v_r, e_p)T_0}{U_0^2 v_r}\right]\frac{1}{\bar{v}}\bar{\nabla}(\bar{g}_1\bar{T})I \\ & + \left[\frac{\mu_{br}}{\rho_p d_p U_0 v_r}\right]\frac{1}{\bar{v}}\bar{\nabla}[(\bar{v}^2\bar{g}_0\bar{T}^{1/2})\bar{\nabla}\cdot\vec{\bar{u}}]I \\ & - \frac{N_0}{\rho_p v_r U_0^2}\frac{1}{\bar{v}}\bar{N}_S I \\ & + 2\left[\frac{\mu_{sr}}{\rho_p d_p U_0 v_r}\right]\frac{1}{\bar{v}}\bar{\nabla}\cdot(\bar{g}_2 T^{1/2}\bar{S}) \\ & - \frac{S_0}{\rho_p v_r U_0^2}\frac{1}{\bar{v}}[\bar{S}_S],\end{aligned} \tag{27}$$

where $\vec{l}$ is the unit vector of the body force and g is the value of the body force per unit mass of bed material, $[S_S]$ is the frictional contribution to the shear stress tensor (the diagonal components are zero), and μ_{br} and μ_{sr} are, respectively, bulk and shear viscosities defined as:

$$\mu_{br} = \rho_p d_p \frac{8}{3\sqrt{\pi}}\eta v_r^2 g_r(v_r) T_0^{1/2}, \tag{28}$$

$$\mu_{sr} = \rho_p d_p g_{2r}(v_r, e_p) T_0^{1/2}. \tag{29}$$

Eq. (27) consists of the following dimensionless groups:

$$\frac{g d_p}{U_0^2},\ \frac{g_{1r}(v_r, e_p)T_0}{U_0^2 v_r},\ \frac{\mu_{br}}{\rho_p d_p U_0 v_r},\ \frac{N_0}{\rho_p v_r U_0^2},\ \frac{\mu_{sr}}{\rho_p d_p U_0 v_r},\ \text{and}\ \frac{S_0}{\rho_p v_r U_0^2}. \tag{30}$$

3.3. Dimensionless energy equation

Inserting Eqs. (17)–(25) into Eq. (3) and considering Eqs. (4)–(6) and Eqs. (8)–(14) gives the following dimensionless energy equation:

$$\begin{aligned}\frac{3}{2}\bar{v}\left(\frac{\partial \bar{T}}{\partial \bar{t}} + \vec{\bar{u}}\cdot\bar{\nabla}\bar{T}\right) = {} & -\left\{\left[\frac{g_{1r}(v_r, e_p)}{v_r}(\bar{g}_1\bar{T}) - \frac{8}{3\sqrt{\pi}}\frac{\eta v_r g_r(v_r) U_0}{T_0^{1/2}}(\bar{v}^2\bar{g}_0\bar{T}^{1/2})\bar{\nabla}\vec{\bar{u}}\right]I \right. \\ & \left. - 2\frac{g_{2r}(v_r, e_p)U_0}{v_r T_0^{1/2}}(\bar{g}_2\bar{T}^{1/2}\bar{S})\right\} : \bar{\nabla}\vec{\bar{u}} \\ & + \bar{\nabla}\left[\frac{g_{3r}(v_r, e_p)T_0^{1/2}}{v_r U_0}(\bar{g}_3\bar{T}^{1/2})\bar{\nabla}\bar{T}\right] \\ & + \bar{\nabla}\left[\frac{g_{4r}(v_r, e_p)T_0^{1/2}}{U_0}(\bar{g}_4\bar{T}^{3/2})\bar{\nabla}\bar{v}\right] \\ & - \frac{g_{5r}(v_r, e_p)T_0^{1/2}}{v_r U_0}(\bar{g}_5\bar{T}^{3/2}).\end{aligned} \tag{31}$$

Eq. (31) involves the following dimensionless groups:

$$\frac{g_{1r}(v_r, e_p)}{v_r},\ \frac{\eta v_r g_r(v_r) U_0}{T_0^{1/2}},\ \frac{g_{2r}(v_r, e_p)U_0}{v_r T_0^{1/2}},\ \frac{g_{3r}(v_r, e_p)T_0^{1/2}}{v_r U_0},\ \frac{g_{4r}(v_r, e_p)T_0^{1/2}}{U_0},\ \text{and}\ \frac{g_{5r}(v_r, e_p)T_0^{1/2}}{v_r U_0}. \tag{32}$$

4. Scale-up relationships

4.1. Dimensionless groups from geometrical and boundary conditions and physical properties of particles and drum wall

The geometrical conditions for solving Eqs. (1)–(3) can be written in terms of the non-dimensional length scales such as L_z/d_p, R/d_p, H_d/d_p and PCT (the drum fill percentage), where H_d is the dam height, L_z is the drum length, and R is the drum radius. The boundary conditions at the drum walls can be given as: $\vec{\bar{u}} \sim \vec{\omega}R/U_0$, $\bar{T} = T_w/T_0$, $\bar{v} = v_w/v_r$, where T_w and v_w are the values of T and v at the drum wall, respectively, and $\vec{\omega}$ is the angular velocity vector of the drum. Note that a symbol '$\sim$' rather than '$=$' is used in giving the wall velocity condition. This is because slippage may occur between the drum wall and the bed material, and there is an axial component of velocity though this is usually very small. For slippage at boundaries, a detailed discussion has been given by Johnson

et al. (1990), Anderson and Jackson (1992) and Nott and Jackson (1992). Considering spherical hard particles that flow across a hard wall surface, balances of force and pseudo-energy (granular temperature) on a vanishingly thin layer of material adjacent to the wall give two equations (boundary conditions). The two equations contain particle-wall slip velocity, restitution coefficient of particles colliding with the wall, angle of friction between particles and wall, and specularity factor etc. (Johnson et al., 1990; Nott & Jackson, 1992). This suggests that the drum-bed material slippage depends on parameters such as restitution coefficient for particle–particle collisions (e_p), restitution coefficient for particle–wall collisions (e_w), particle surface frictional coefficient (μ_p), wall surface frictional coefficient (μ_w), particle surface roughness (Δ_p) and wall surface roughness (Δ_w) (specularity factor measures the fraction of the momentum of the incident particles transferred to the wall, which is a function of the above parameters). If the deformation of particles and drum wall is not negligible during collisions, particle elasticity modulus (E_p) and wall elasticity modulus (E_w) have to be taken into account. For non-spherical particles, particle shape factor (s) has to be included. For drums with an inclination, an inclination angle θ should be accounted for. Because the axial direction particle velocity is a function of feed rate (which may be independent of drum rotational speed), the average axial flow velocity, w, should be included. As a consequence, besides the parameters obtained in Section 3, the following dimensionless numbers should be considered:

$$\omega R/w, L_z/d_p, H_d/d_p, R/d_p, \text{ PCT, } s, e_p, e_w, \mu_p, \mu_w, \Delta_p/d_p, \Delta_w/d_p, N_0/E_p, N_0/E_w, \text{ and } \theta. \quad (33)$$

It is noted that the restitution coefficients may be linked to other physical properties such as elasticity modulus, friction coefficient and surface roughness. However, they are regarded as independent parameters in the present work because no general relationship for such a link has been found in the literature.

4.2. Dimensionless parameter due to diffusion

As mono-sized particles are considered, the diffusion here only refers to self-diffusion. Assuming that the distribution of granular temperature is isotropic, the self-diffusivity D_s could be expressed as (Hsiau & Hunt, 1993):

$$D_s = \frac{d_p\sqrt{\pi T}}{8(e_p+1)\nu g_0(\nu)}. \quad (34)$$

Self-diffusion is expected to be partly responsible for the spread of residence time distribution of particles. Eq. (34) can be rearranged to give:

$$D_s/D_{s0} = \frac{\sqrt{\bar{T}}}{\bar{\nu}\bar{g}_0}, \quad (35)$$

where

$$D_{s0} = \frac{d_p\sqrt{\pi T_0}}{8(e_p+1)v_r g_r(v_r)}. \quad (36)$$

Eq. (36) defines a dimensionless group similar to the Peclet number:

$$Pe_0 = \frac{D_{s0}}{d_p\sqrt{T_0}}. \quad (37)$$

More discussion of particle diffusion will be given in Section 4.8.3.

4.3. Dimensionless parameter due to particle size distribution

For granular material with wide size distribution (other physical properties being the same), particles are usually divided into different groups, each of which has a relatively narrow size spread and can be termed as a phase (in the kinetic sense). In this case, Eqs. (1)–(3) have to be modified to account for interactions between different phases. This is beyond the scope of this paper and will not be discussed further. However, for scale-up purpose, a dimensionless size distribution is required.

4.4. Controlling dimensionless groups

As can be seen from above, there are over 20 dimensionless groups. However, not all of them are independent. First of all, the solid volumetric fraction depends on the operating conditions of the drum, physical properties of the granular material and drum wall, drum geometry as well as the drum fill level. The ratio of U_0^2 to T_0 has been accounted for in Eq. (30). As a consequence, the dimensionless groups given in Eqs. (32) and (37) are not controlling parameters because they can be derived from the parameters given in Eq. (30). Secondly, due to the Coulomb frictional law, only one of $N_0/\rho_p v_r U_0^2$ and $S_0/\rho_p v_r U_0^2$ can be regarded as independent (the friction coefficient has been accounted for in Eq. (33)). We arbitrarily choose $N_0/\rho_p v_r U_0^2$ as an independent group. Finally, comparison of Eqs. (28) and (29) suggests that $g_{1r}(v_r, e_p)T_0/U_0^2 v_r$, $\mu_{br}/\rho_p d_p U_0 v_r$, and $\mu_{sr}/\rho_p d_p U_0 v_r$, are interdependent. We also arbitrarily choose $\mu_{sr}/\rho_p d_p U_0 v_r$ as an independent group. As a consequence, the controlling non-dimensional parameters can be identified as:

$$\frac{gd_p}{U_0^2}, \frac{N_0}{\rho_p v_r U_0^2}, \frac{\mu_{sr}}{\rho_p d_p U_0 v_r}, \omega R/w, L_z/d_p, H_d/d_p, R/d_p, \text{PCT, } s, e_p, e_w, \mu_p, \mu_w, \Delta_p/d_p, \Delta_w/d_p, N_0/E_p, N_0/E_w, \theta \text{ and particle size distribution.} \quad (38)$$

The term gd_p/U_0^2 is the modified Froude number which compares the inertial force with body force (e.g. gravity). This group has been used intensively in the literature; see for examples Henein et al. (1983), Rutgers

(1965) and Zablotny (1965). The term $N_0/\rho_p v_r U_0^2$ compares the normal stress due to friction with the inertial force and is called 'pseudo-Euler number' as it is similar to the Euler number used in fluid mechanics defined as $E_u = \Delta P/1/2\rho_f U_{fo}^2$, where ΔP, ρ_f and U_{fo} are pressure drop, density and characteristic velocity of the fluid, respectively. The term $\mu_{sr}/\rho_p d_p U_0 v_r$ compares the force due to the collisional contribution (similar to viscous force) with the inertial force and is called the 'pseudo-Reynolds number due to its similarity to the Reynolds number used in fluid flows. Other terms given above are self-explanatory.

The reference values of the parameter U_0, N_0 and v_r in Eq. (38) can be taken as: $U_0 =$ linear velocity of drum wall, $N_0 = \rho_p v_r g H_m$ (H_m is the bed depth at the mid-chord position), and v_r=solids volumetric fraction under closely packed conditions.

4.5. Quasi-static flow regime

In the quasi-static flow regime, the deformation of granular material is slow, and the velocity fluctuation and hence the granular temperature is negligible. From Eq. (29), it is seen that the term $\mu_{sr}/\rho_p d_p U_0 v_r$ is negligible, and the controlling parameters become:

$$gd_p/U_0^2, N_0/\rho_p v_r U_0^2, \omega R/w, L_z/d_p, H_d/d_p, R/d_p,$$
$$\text{PCT}, s, e_p, e_w, \mu_p, \mu_w, \Delta_p/d_p, \Delta_w/d_p, N_0/E_p,$$
$$N_0/E_w, \theta \text{ and size distribution.} \quad (39)$$

4.6. Rapid granular flow regime

In the rapid granular flow regime, the granular material is fully dynamic, and the frictional contribution to the total stress is negligible. The term $N_0/\rho_p v_r U_0^2$ is therefore neglected and the governing parameters become:

$$\frac{gd_p}{U_0^2}, \frac{\mu_{sr}}{\rho_p d_p U_0 v_r}, \omega R/w, L_z/d_p, H_d/d_p, R/d_p,$$
$$\text{PCT}, \ s, e_p, e_w, \mu_p, \mu_w, \Delta_p/d_p, \Delta_w/d_p, N_0/E_p,$$
$$N_0/E_w, \theta \text{ and size distribution.} \quad (40)$$

4.7. Dependent variables

When all the independent non-dimensional groups are set, the dependent variables are fixed. The dependent variables include particle velocity throughout the material bed, the solid volumetric fraction distribution, and the granular temperature. As particle residence time depends on the particle velocity distribution, the drum geometry and the diffusivity, which is a function of granular temperature and physical properties of the granular material, the particle residence time distribution (RTD) is also a dependent variable.

If two drums are designed and operated to have identical values of all the controlling dimensionless groups, then the dependent non-dimensional variables of the two drums must also be identical at every location within the drums (Kline, 1965). The variables include v/v_r, $\vec{u}/U_0$, T/T_0, and $\tau U_0/d_p$, where τ is the average residence time.

4.8. Discussion on other dimensionless groups appearing in the literature

Several other dimensionless groups have appeared in the literature. These include (1) the Bagnold number (Hill, 1966), which indicates the relative importance of the particle–particle interaction and the viscous force; (2) the pseudo-Knudsen number (Savage, 1998), which is a measure of the energy dissipation of granular flow systems due to inelasticity and finite roughness of particles; (3) the Sa number obtained by Savage (1984) through dimensional analysis, and (4) the Peclet number used in the axial dispersion model for particle residence time distribution and heat transfer (Fan & Ahn, 1961; Abouzeid et al., 1974; Sullivan & Sabersky, 1975; Patton et al., 1986; Hunt, 1991; Natarajan & Hunt, 1997). As the focus of this work is on cases where the effect of interstitial fluid is negligible, only Sa number, pseudo-Knudsen number and Peclet number are discussed in the following.

4.8.1. Sa number

Sa number compares the collisional contribution with the total normal stress, and is defined as:

$$Sa = \frac{\rho_p d_p^2 (\mathrm{d}v/\mathrm{d}y)^2}{N_T}, \quad (41)$$

where $\mathrm{d}v/\mathrm{d}y$ is the characteristic velocity gradient across the shear layer, and N_T is the characteristic normal stress of the shear layer. For one-dimensional Couette flows with constant granular temperature T_t, the relationship between the velocity gradient and the granular temperature can be given as (Bagnold, 1954):

$$T_t = F(v, \eta, d_p) \left(\frac{\mathrm{d}v}{\mathrm{d}y}\right)^2, \quad (42)$$

where $F(v, \eta, d_p)$ is a function of v, η and d_p and may take different forms (Bagnold, 1954; Lun et al., 1984). The expression from Lun (1984) is adopted here, see also Ding, Forster, Seville, and Parker (2000):

$$F_p(v, \eta, d_p) = \frac{5\pi d_p^2}{4608\eta(1-\eta)v^2 g_0(v)} \left\{ \frac{1 + 8/5\eta(3\eta - 2)v g_0(v)}{(2-\eta)\eta g_0(v)} \times \left[1 + \frac{8}{5}\eta v g_0(v)\right] + \frac{768}{25\pi}\eta v^2 g_0(v) \right\}. \quad (43)$$

Combination of Eqs. (41), (42) and (43) suggests that the Sa number can be derived from the dimensionless groups derived in this work, i.e. $N_0/\rho_p v_r U_0^2$ and $\mu_{sr}/\rho_p d_p U_0 v_r$. Small Sa numbers ($< 0.1$) correspond to relatively large pseudo-Euler numbers, i.e. the stresses generated by Coulomb dry frictional interactions are dominant (quasi-static flow regime). Large values (close to unity) of Sa number correspond to relatively large pseudo-Reynolds numbers, i.e. particles collide vigorously and nearly instantaneously and the generation of stresses is primarily by collisional interactions (rapid granular flow regime). In the following, the order of magnitude of Sa number for granular flow in rolling mode rotating drums operated at low to medium rotational speeds will be evaluated.

For rolling mode rotating drums operated at low to medium rotational speeds, the profile of velocity parallel to the bed surface is approximately parabolic, see for example Khakhar, McCarthy, Shinbrot, and Ottino (1997) and Elperin and Vikhansky (1998). If the free surface condition is applied, the following expression can be obtained (Ding, Forster, Seville, & Parker, 2001a):

$$v = \frac{\omega(h+\delta)}{1-\Lambda^2}\left[\Lambda^2 - \left(\frac{y}{\delta}\right)^2\right], \tag{44}$$

where ω is the angular velocity of the drum, h is the shortest distance between the drum centre and bed surface, y is the depth from the bed surface, δ is the active layer depth, and Λ is a parameter depending on the rheological properties of the granular material (Fig. 1). The parameter Λ is a function of position x and usually lies within 0.75 –0.9 for $x/(2L) = 0.1$–0.9, while the active layer depth can be estimated by using the following expression (Ding et al., 2001a):

$$\delta = \frac{1}{3\Lambda^2+1} \times \left[\sqrt{6(1-\Lambda^2)(3\Lambda^2+1)\left(Lx - \frac{x^2}{2}\right) + 4h^2} - 2h\right], \tag{45}$$

where L is the half chord length of the bed.

Considering the mid-chord position ($x = L$), then the active layer depth can be given as:

$$\delta_m = \frac{1}{3\Lambda_m^2+1}[\sqrt{3(1-\Lambda_m^2)(3\Lambda_m^2+1)L^2 + 4h^2} - 2h], \tag{46}$$

where $\Lambda_m = \Lambda_{|x=L}$. The maximum velocity gradient in the mid-chord position is obtained from Eq. (44):

$$\left(\frac{\mathrm{d}v}{\mathrm{d}y}\right)_m = -\frac{2\omega(h+\delta_m)}{(1-\Lambda_m^2)\delta_m}. \tag{47}$$

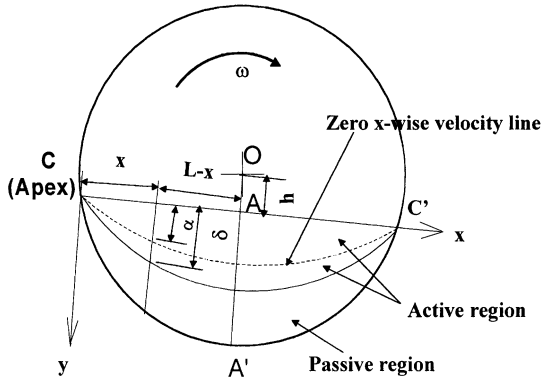

Fig. 1. Schematic representation of the transverse plane of a rolling mode rotating drum.

The characteristic normal stress can be estimated as:

$$N_T = \delta_m \rho_p v_r g. \tag{48}$$

Combination of Eqs. (41), (47) and (48) gives:

$$Sa = \frac{4}{v_r(1-\Lambda_m^2)^2}\left(\frac{\omega^2 R}{g}\right)\left(\frac{d_p}{R}\right)\left(\frac{d_p}{\delta_m}\right)\left(1+\frac{h}{\delta_m}\right)^2. \tag{49}$$

Eq. (49) suggests that Sa number depends on the rheological properties of granular material through parameter Λ, the drum operating conditions through the Froude number ($\omega^2 R/g$), v_r, dimensionless particle size d_p/R, and the drum fill level through h/δ_m. Fig. 2 shows the calculated Sa number under typical laboratory and industrial conditions. It can be seen that the granular flow in large rotating drums operated at low to medium rotational speeds is in the quasi-static regime, while the flow of relatively large particles in small drums operated at medium rotational speeds may be in the transition regime.

4.8.2. Pseudo-Knudsen number

The pseudo-Knudsen number is defined as:

$$K_{np} = \left|\frac{(\mathrm{d}v/\mathrm{d}y)d_p}{T_c^{1/2}}\right| \tag{50}$$

where T_c is the characteristic granular temperature of the system. As mentioned earlier, K_{np} is a measure of energy dissipation of the granular system. It is therefore also an indication of the adequacy of the granular flow kinetic theory which can be considered as perturbations of the case of perfectly elastic particles. Consequently, the dissipation of the granular flow system and hence the pseudo- Knudsen number has to be small for the constitutive relationships for $\vec{P}_R$, γ and Γ given in Section 2 to be valid.

It is noted that if the dissipation of the granular flow system is very high so that the granular temperature

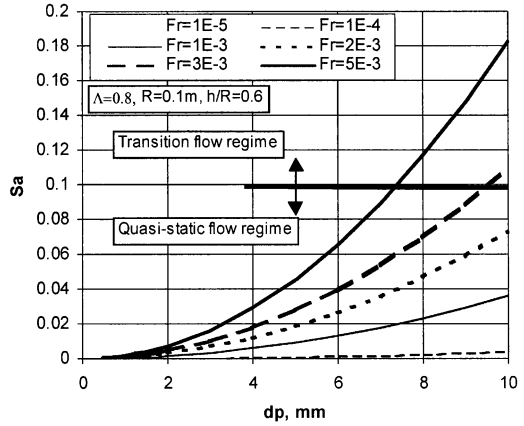

(a) 0.2m diameter drum

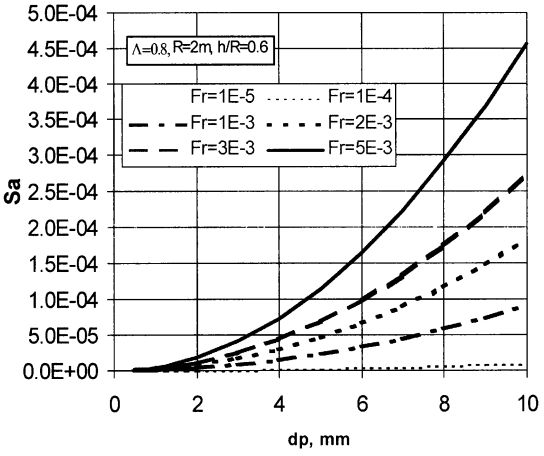

(b) 4m diameter drum

Fig. 2. Sa number under various conditions, $v_r = 0.5$.

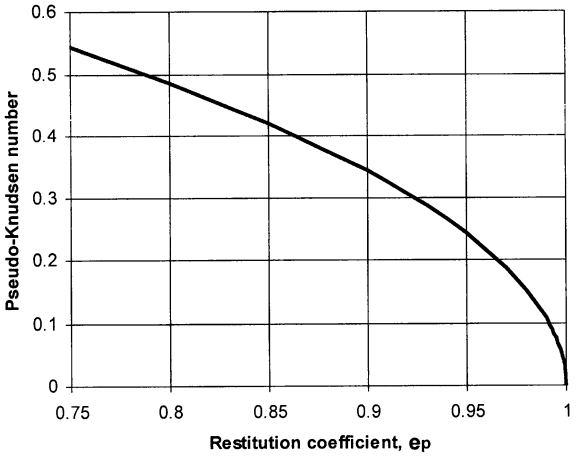

Fig. 3. Effect of particle restitution coefficient on the pseudo-Knudsen number. $v_m = 0.65$, $v = 0.5$.

approaches zero, K_{np} goes to infinity, and the kinetic theory collapses. However, this does not affect the results obtained in the above sections as the frictional contribution dominates in this case. In the following, the order of magnitude of K_{np} for granular flow in rotating drums is evaluated.

As granular flows in a rolling mode rotating drum are somewhat similar to one-dimensional horizontal flow formed by two opposite plane shear stresses imposed on the top and bottom of the boundaries (Ding et al., 2000), T_c in Eq. (50) can be approximately taken as T_t given in Eq. (42). Combination of Eqs. (42), (43) and (50) gives:

$$K_{np} = \frac{d_p}{\sqrt{F(v,\eta,d_p)}} = \frac{\sqrt{4608\eta(1-\eta)v^2 g_0(v)}}{\sqrt{5\pi\cdot\{\dfrac{1+8/5\eta(3\eta-2)vg_0(v)}{(2-\eta)\eta g_0(v)}[1+\dfrac{8}{5}\eta v g_0(v)]+\dfrac{768}{25\pi}\eta v^2 g_0(v)\}}} \tag{51}$$

Eq. (51) suggests that K_{np} is a function of v and e_p through η. As v is not far from 0.5, K_{np} is mainly affected by e_p. Fig. 3 shows such dependence. It can be seen that the dense-gas kinetic theory is only applicable to granular materials with high restitution coefficients. However, this is not very strict as mentioned in Section 2.2.

4.8.3. Peclet number

The Peclet number is usually used in the analyses of axial particle dispersion and heat transfer in granular flows. In the former case, it is defined as (Fan & Ahn, 1961; Abouzeid et al., 1974; Wes, Drinkenburg, & Stemerding, 1976):

$$Pe_x = wL_Z/D_e, \tag{52}$$

where D_e is the axial dispersion coefficient. For heat transfer analysis, D_e in Eq. (52) is replaced by the thermal diffusivity (Sullivan & Sabersky, 1975; Patton et al., 1986; Hunt, 1991; Natarajan & Hunt, 1997).

As shown in Section 4.2, the particle diffusion coefficient is a function of the granular temperature (if it is isotropic, Eq. (34)). From Eq. (29), the shear viscosity is also a function of the granular temperature. Consequently, the Peclet number defined by Eq. (52) can be derived from $\mu_{sr}/\rho_p d_p U_0 v_r$, $\omega R/w$, L_z/d_p and R/d_p.

In real granular flows, the granular temperature may be anisotropic (due to the streaming granular temperature), see for example Campbell (1990) and Hsiau and Shieh (2000). In rotating drums, the dispersion coefficient in the axial direction is often several orders of magnitude smaller than that in the transverse plane (Boateng & Barr,

1997; Fan & Ahn, 1961). This, however, should not affect the results of this work as the diffusivity is often a function of the operating conditions and particle physical properties which have already been accounted for by the dimensionless groups shown in Eq. (38).

4.9. Limitations of the scaling relationships

The scale-up relationships described above are only as valid as the governing equations. The governing equations presented in Section 2.2 are for cohesionless particles and only for cases where the effect of interstitial fluid is negligible. They may not be applicable to very small particles (e.g. $< \sim 100\,\mu m$) and the cataracting and centrifuging modes as the fluid–solid interaction may be important in these cases.

For cohesive particles, inter-particle forces are important. Similarity will not exist, nor are the controlling dimensionless groups given in the previous sections complete, when such inter-particle forces are important.

For rotating drums operated at elevated temperatures, a thermal energy conservation equation should be included which will give some other dimensionless groups. However, scale-up is extremely difficult for drums operated at > 500–$800^{\circ}C$ due to strong non-linearity of radiative heat transfer.

As mentioned in Section 4.8, the granular flow kinetic theory only applies to low pseudo-Knudsen numbers. As a consequence, in the rapid granular flow regime, the scale-up relationships may not be appropriate for materials with very low restitution coefficients (e.g. < 0.6).

5. Initial experiments and future work

5.1. Initial experimental work

As can be seen from Section 4.4, there are about 19 controlling dimensionless numbers. Initial experiments were therefore carried out to explore the possibility of combining some of these groups so that the total number of effective controlling dimensionless groups could be reduced. The methodology for this was by examining particle velocity distribution in the rolling mode and the transition criteria between the slumping and rolling modes. The experiments were conducted with three drums ($2R =$ 200, 240 and 400 mm ID, and 1000 mm long). Sand (450–550 μm, average 500 μm), glass beads (1.5, 3.0 and 4.0 mm) and titanium dioxide particles (1.0–1.4 mm, average 1.2 mm) were tested. To avoid particle-drum wall slippage, a layer of sand paper (grit 36) was glued to the drum walls but not end plates which were made of aluminium. The drums were operated in batch mode and the positron emission particle tracking (PEPT) technique was used to follow a tracer particle trajectory. The trajectory was then used to calculate the particle velocity field and slumping frequency (solids motion is in a rolling mode only when the tracer has one slump when moving down the bed surface). A detailed description of the PEPT technique is available elsewhere (Parker, Broadbent, Fowles, Hawkesworth, & McNeil, 1993, 1997; Forster, Seville, Parker, & Ding, 2001).

The experimental results for the slumping–rolling transition are shown in Table 1. The data in the last two rows are from Henein et al. (1983) for purpose of comparison. From Table 1, the following conclusions could be obtained:

(a) For a given granular material and a drum fill percentage, the slumping–rolling transition occurs approximately at the same modified Froude number (Rows 1 and 6 for sand and Rows 2–4 for glass beads, last column), in agreement with Henein et al. (1983).
(b) The ratio of drum length to particle diameter, L_z/d_p, has little effect on the slumping–rolling transition in the range of 250–920 (Rows 1 and 6 for sand and Rows 2–4 for glass beads, Column 5). This conclusion may not be applicable to continuous operations as L_z/d_p may affect the residence time distribution. More work is required in this aspect.

For rotating drums operated in a rolling mode, the surface velocity distributions of free-flowing materials are approximately parabolic under certain conditions (i.e. nearly spherical particles with relatively high restitution coefficient and the fill level is not too low, Boateng & Barr, 1997). It follows that, for a given drum and drum fill percentage, surface velocity profiles should be uniquely determined by the maximum surface velocity under these conditions. As a consequence, only the maximum surface velocity was extracted from the PEPT data of the initial experiments. Fig. 4 shows the dependence of dimensionless maximum surface velocity on Froude number under various conditions. Here the dimensionless surface velocity is defined as (Ding et al., 2001b):

$$\bar{V}_m = \left(\frac{V_m}{e_p \omega L \sin\beta}\right)\sqrt{\frac{d_p}{D}}, \tag{53}$$

where V_m is the maximum surface velocity and β is the dynamic repose angle. The derivation of Eq. (53) is simply based on the following arguments: (a) The maximum surface velocity, V_m, is proportional to $(L \sin\beta)$ due to conversion of potential energy to kinetic energy. (b) An increase in drum rotational speed increases the surface velocity, and (c) A high e_p implies low kinetic energy dissipation and hence a high surface velocity. Combination of (a)–(c) gives:

$$V_m \propto e_p^a \omega^b (L \sin\beta)^c \tag{54}$$

where a, b, and c are constants. However, Eq. (54) gave a poor fit to the experimental results for $a = 0-2$, and $b = c = 0-2$ (here $b = c$ is for dimensional harmony). Inspired

Table 1
Transition from slumping to rolling modes (PCT = 10%)

Material	D, m	L_z, m	d_p, m	L_z/d_p	D/d_p	Fr	$Fr\sqrt{D/d_p}$
Sand	0.20	0.3	5×10^{-4}	600	400	9.5×10^{-5}	1.9×10^{-3}
Glass beads	0.40	1.0	4×10^{-3}	250	100	1.5×10^{-5}	1.51×10^{-4}
Glass beads	0.40	1.0	3×10^{-3}	333	133	1.4×10^{-5}	1.61×10^{-4}
Glass beads	0.40	1.0	1.5×10^{-3}	667	267	8.9×10^{-6}	1.45×10^{-4}
TiO_2	0.24	1.0	1.2×10^{-3}	833	200	4.3×10^{-4}	6.1×10^{-3}
Sand B[a]	0.40	0.46	5×10^{-4}	920	800	6.8×10^{-5}	1.9×10^{-3}
Limestone B[a]	0.40	0.46	4.3×10^{-3}	107	93	6.8×10^{-4}	6.6×10^{-3}

[a]Data from Henein et al. (1983).

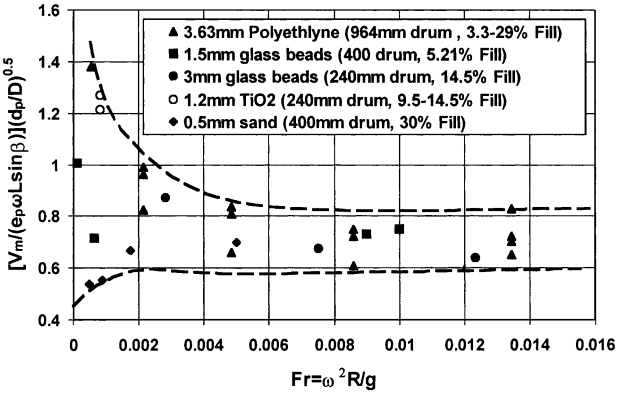

Fig. 4. Dimensionless maximum surface velocity as a function of Froude number.

by the work of Henein et al. (1983), the group $(d_p/D)^n$ was added to Eq. (54). The power n was examined in the range of $-2 \sim +2$ and 0.5 was found to give the best fit when $a = b = c = 1$. This leads to Eq. (53). The power of d_p/D agrees with the results obtained by Henein et al. (1983) in their work on slumping–rolling transition.

Eq. (53) contains a parameter 'dynamic repose angle' which is not included in the controlling dimensionless groups, Eq. (38). However, this parameter depends mainly on the physical properties of particles if there is no slippage at the drum wall. The effects of drum operating conditions such as fill percentage and rotational speed are very small under typical industrial conditions (Spurling, 2000). In constructing Fig. 4, the dynamic repose angles of granular materials are 26.5° for glass beads, 33° for sand, 32° for titanium dioxide, and 25° for polyethylene. The values for the former three materials were obtained from the PEPT measurements (i.e. calculated from the maps of velocity vectors or the occupancy plots, see Forster et al. (2001), and Ding et al. (2001a)), while the value for polyethylene is from Boateng and Barr (1997). The restitution coefficients are taken as 0.95 for glass beads (Hoomans, 2000), 0.85 for polyethylene (Boateng & Barr, 1997), 0.75 for sand (estimated) and 0.7 for titanium dioxide (estimated). The estimation of e_p for sand and TiO_2 particles was carried out by comparing the rebound heights of sand or titanium dioxide particles with those of glass beads when dropping down to a steel plate from the same height:

$$(e_p)_1 = (e_p)_0 \sqrt{\frac{(h_r)_1}{(h_r)_0}}, \tag{55}$$

where h_r is the rebound height, and subscripts 0 and 1 denote, respectively, glass beads and sand or titanium dioxide particles (The square root comes from the relationship between velocity and height). This method is not rigorous but is believed to give a reasonable estimation. For further information on the theories and experimental techniques for the measurement of the restitution coefficient, see for example, Goldsmith (1960), Maw, Barber, and Fawcett (1981), Sondergaard, Chaney, and Brennen (1990), and more recently, Boateng and Barr (1997), Gorham and Kharaz (1999) and Hoomans (2000).

The data for glass beads and sand as shown in Fig. 4 were selected in such a way that the surface velocity profiles were parabolic (in fact, parabolic profiles were observed in most experiments at low to medium rotational speeds). Experiments with the titanium dioxide particles showed that the surface velocity profiles had two peaks positioned at $x/(2L) \sim 0.3$ and 0.7, respectively, with the first peak being a magnitude of about 10% lower than the second one. The data points in Fig. 4 for titanium dioxide were calculated based on the higher peak. The data for polyethylene particles from Boateng and Barr (1997) are also included for comparison. It can be seen that the dimensionless maximum surface velocity tends to be a constant when the Froude number is greater than ~ 0.003. This indicates that there may exist a self-mimicking zone and the criterion for the self-mimicking zone is different from that for the slumping–rolling transition (Table 1). Fig. 4 also suggests that the criterion for the self-mimicking zone is independent of the ratio of drum length to particle diameter (L_z/d_p) and the relative drum surface roughness ($\Delta_w/d_p, \Delta_{wp}$ is fixed in all runs). As $\bar{V}_m$ tends to be a constant at $Fr > 0.003$, Eq. (53) indicates that the Froude number ($\omega^2 R/g$), diameter ratio (D/d_p), drum fill percentage through $L/D[= (L/d_p)/(D/d_p)]$, and particle

restitution coefficient (e_p) can be combined to give one dimensionless parameter, a possibility of reducing the total number of controlling dimensionless groups. It is to be noted that, in Fig. 4, the data points at $Fr > 0.003$ correspond to parabolic surface velocity profiles, and the data points for titanium dioxide particles are located at $Fr < 0.001$.

5.2. Future work

Future work should involve the following three groups of experiments:

(a) Group I: examination of the effects on the dependent parameters of drum operating conditions including gd_p/U_0^2, $N_0/\rho_p v_r U_0^2$, $\mu_{sr}/\rho_p d_p U_0 v_r$, $\omega R/w$, and PCT. The task of this group will be conducted in at least three drums operated both in batch and continuously. These drums will be constructed to have high wall friction coefficient (to avoid wall slippage) and will be geometrically similar. Spherical hard particles with high restitution coefficient will be used. Experiments of this group will also involve the verification of criteria for the transition from quasi-static to rapid flow regimes (Section 4.8.1).
(b) Group II: examination of the effects on the dependent parameters of physical properties of both particles and drum wall including $\Delta_w/d_p, \Delta_p/d_p, e_w, e_p, \mu_p, \mu_w, s, N_0/E_p, N_0/E_w$ and particle size distribution. The task of this group will be conducted with one drum diameter but using different sized- and shaped-particles, and various surface roughness of particles and drum wall (e.g. using different sand papers). Batchwise operations will be adopted.
(c) Group III: examination of the effects on the dependent parameters of drum geometry including L_z/d_p, H_d/d_p, R/d_p, and θ. The task of this group will be carried out with two or more drums. Both batchwise and continuous operations will be adopted.

The dependent parameters include v/v_r, $\vec{u}/U_0$, T/T_0, and $\tau U_0/d_p$, where $\tau U_0/d_p$ is unimportant for batchwise operations. Positron Emission Tomography (PET) will be used to measure the RTDs, while the PEPT technique will be used to map the fields of particle velocity, granular temperature and the solids volumetric fraction.

6. Conclusions

The scaling relationships for rotating drums have been derived in this paper. This was achieved by non-dimensionalising the differential equations that govern solids motion within them. The controlling dimensionless groups were identified as Froude number, pseudo-Reynolds number, pseudo-Euler number, drum geometric ratios, drum inclination, drum fill percentage, size distribution of particles, and physical properties of particles and the drum wall such as restitution coefficient and elasticity modulus. At relatively low pseudo-Reynolds numbers, the effect of velocity fluctuation and hence the granular temperature could be neglected, with the granular flows lying in the quasi-static regime. At relatively low pseudo-Euler numbers, the effect of frictional contribution to the total stress is negligible, and the flow is therefore in the rapid granular flow regime. It has been shown that granular flows in large drums operated at low to medium rotational speeds are often in the quasi-static regime, while those in small drums operated at medium rotational speeds may be in the transition flow regime. It has also been shown that granular flow kinetic theory is only valid for granular materials with relatively high restitution coefficients. Preliminary experimental work has been carried out with the aim at reducing the total number of controlling parameters. The results show that the Froude number, particle-to-drum diameter ratio, drum fill percentage, and particle restitution coefficient can be combined to give a single dimensionless parameter if drums are operated in a rolling mode and the Froude number is greater than 0.003.

Notation

a, b, c	constants, Eq. (54), dimensionless
d_p	particle diameter, m
D_e	axial particle dispersion coefficient, m^2/s
D_s	particle self-diffusivity, m^2/s
D_{so}	reference value of D_s, m^2/s
e_p	particle restitution coefficient, dimensionless
e_w	restitution coefficient of the drum wall, dimensionless
E_p	particle elasticity modulus, N/m^2
E_u	Euler number, dimensionless
E_w	drum wall elasticity modulus, N/m^2
$\vec{F}$	body force vector, N/kg
F_S	constant in Eq. (16), N/m^2
$F(v, \eta, d_p)$	see Eq. (43) for definition, m^2
g	value of the body force per unit mass, N/kg
$g_0(v)$	see Eq. (9) for definition, dimensionless
$g_r(v_r)$	$\equiv g_0(v_r)$, dimensionless
$\bar{g}_0$	$\equiv g_0(v)/g_r(v_r)$, dimensionless
$g_{ir}(v_r, e_p)$	$i = 1$–5, see Eqs. (10)–(14) for definition, dimensionless
$g_{ir}(v_r)$	$g_i(v_r, e_p)$, dimensionless
$\bar{g}_i$	$\equiv g_i(v, e_p)/g_{ir}(v_r, e_p)$, dimensionless
h	shortest distance between drum centre and bed surface, m
h_r	rebound height, m

H_d dam height, m
H_m bed depth at mid-chord position, m
I identity matrix, dimensionless
K_{np} pseudo-Knudsen number, dimensionless
$\vec{l}$ unit vector, dimensionless
L half chord length, m
L_z drum length, m
n_1 constant in Eq. (16)
n_2 constant in Eq. (16)
N_0 reference normal stress, N/m^2
N_S frictional contribution to the total normal stress, N/m^2
N_T normal stress due to the frictional contribution (Eq. (48)), N/m^2
$\bar{N}_S$ dimensionless normal stress due to the frictional contribution, dimensionless
ΔP pressure drop, Pa
PCT drum fill percentage, dimensionless
Pe_o Peclet number based on self-diffusivity, dimensionless
Pe_x Peclet number (axial direction), dimensionless
$\vec{P}_R$ kinetic and collisional contributions to the total stress tensor, N/m^2
$\vec{P}_S$ frictional contribution to the total stress tensor, N/m^2
R drum radius, m
s particle shape factor, dimensionless
S_a Savage number, dimensionless
S_0 reference shear stress, N/m^2
S deviatoric part of the rate of deformation tensor, see Eq. (8), 1/s
$\bar{S}$ dimensionless deviatoric part of the rate of deformation tensor, dimensionless
S_S frictional contribution to the shear stress, N/m^2
$\bar{S}_S$ dimensionless shear stress due to the frictional contribution, dimensionless
$[S_S]$ frictional contribution to the shear stress tensor, N/m^2
t time, s
$\bar{t}$ dimensionless time, dimensionless
T granular temperature, m^2/s^2
T_0 reference granular temperature, m^2/s^2
T_c granular temperature (Eq. (50)), m^2/s^2
T_t granular temperature (Eq. (42)), m^2/s^2
T_w granular temperature at the drum wall, m^2/s^2
$\bar{T}$ dimensionless granular temperature, dimensionless
$\vec{u}$ velocity vector, m/s
$\vec{\bar{u}}$ dimensionless velocity vector, dimensionless
U_{fo} velocity of the fluid, m/s
U_0 reference velocity, m/s
v solids velocity in the shear layer parallel to bed surface, m/s
V_m maximum surface velocity, m/s
$\bar{V}_m$ dimensionless maximum surface velocity, dimensionless
w average axial flow velocity, m/s
y y-direction co-ordinate

Greek letters

α distance from zero x-direction velocity line to bed surface, m
β dynamic repose angle, rad
δ active layer depth of the rolling mode rotating drum, m
δ_m active layer depth at the mid-chord position, m
Δ_p particle surface roughness, m
Δ_w wall surface roughness, m
ϕ frictional angle, $\circ$
γ specific pseudo-thermal energy dissipation, J/m^3 s
Γ pseudo-thermal energy flux, J/m^2 s
η $\equiv (1+e_p)/2$
Λ $\equiv \alpha/\delta$, dimensionless
Λ_m value of Λ at the mid-chord position, dimensionless
μ_p frictional coefficient of the particle surface, dimensionless
μ_w frictional coefficient of the drum wall surface, dimensionless
μ_{br} bulk viscosity, Pa s
μ_{sr} shear viscosity, Pa s
ν solid volumetric fraction, dimensionless
$\bar{\nu}$ $\equiv \nu/\nu_r$, dimensionless
ν_m maximum shearable solid volumetric fraction, dimensionless
$\nu_{\min}$ value of ν when evenly distributed particles no longer touch, dimensionless
ν_r reference solid volumetric fraction, dimensionless
ν_w value of ν at the drum wall, dimensionless
θ inclination of the drum, $^\circ$
ρ bulk density of granular material, kg/m^3 (bed)
ρ_f density of fluid, kg/m^3
ρ_p particle material density, kg/m^3 (particle)
τ average residence time, s
ω angular velocity, rad/s
$\vec{\omega}$ angular velocity vector, rad/s

Acknowledgements

Financial support from EPSRC, Huntsman Tioxide and United Biscuits is gratefully acknowledged. The authors also acknowledge the helpful comments of Professor

J. F. Davidson and Dr. D. M. Scott of the University of Cambridge.

References

Abouzeid, A.-Z. M. A., Mika, T. S., Sastry, K. V., & Fuerstenau, D. W. (1974). The influence of operating variables on the residence time distribution for material transport in a continuous rotary drum. *Powder Technology*, *10*, 273–288.

Anderson, K. G., & Jackson, R. J. (1992). A comparison of the solutions of some proposed equations of motion of granular materials for fully developed flow down inclined planes. *Journal of Fluid Mechanics*, *241*, 145–168.

Bagnold, R. A. (1954). Experiments on a gravity free dispersion of large solid spheres in a Newtonian fluid under shear. *Proceedings of the Royal Society*, *225*, 49–63.

Boateng, A. A., & Barr, P. V. (1997). Granular flow behaviour in the transverse plane of a partially filled rotating cylinder. *Journal of Fluid Mechanics*, *330*, 233–249.

Campbell, C. S. (1990). Rapid granular flows. *Annual Review of Fluid Mechanics*, *22*, 57–92.

Cleary, P. W., Metcalfe, G., & Liffman, K. (1998). How well do discrete element granular flow models capture the essentials of mixing processes? *Applied Mathematical Modelling*, *22*, 995–1008.

Cowin, S. C. (1974). A theory for the flow of granular materials. *Powder Technology*, *9*, 61–69.

Ding, Y. L., Forster, R., Seville, J. P. K., & Parker, D. J. (2000). Particle segregation in rapid granular flows, *Particle Technology UK Forum*, 1–2 September, Aston University, UK.

Ding, Y. L., Forster, R. N., Seville, J. P. K., & Parker, D. J. (2001a). Solids motion in rolling mode rotating drums operated at low to medium rotational speeds. *Chemical Engineering Science*, *56*, 1769–1780.

Ding, Y. L., Forster, R. N., Seville J. P. K., & Parker, D. J. (2001b). Surface motion of granular materials in the rolling mode rotating drums. *Powder Technology*, submitted for publication.

Drake, T. D. (1988). Experimental flows of granular material. Ph.D. dissertation, University of California, Los Angeles, California, USA.

Elperin, T., & Vikhansky, A. (1998). Granular flow in a rotating cylindrical drum. *Europhysics Letters*, *42*, 619–623.

Fan, L. S., & Ahn, Y. K. (1961). Axial dispersion of solids in rotary solid flow systems. *Applied Science Research (Section A)*, *10*, 465–470.

Forster, R. N., Seville, J. P. K., Parker, D. J., & Ding, Y. L. (2001). Tracking single particles in process equipment or probing processes using positrons. *KONA Powder and Particle*, *18*, 139–148.

Goldsmith, W. (1960). Impact, the theory and physical behaviour of colliding solids, London: E. Arnold Publishers.

Gorham, D. A., & Kharaz, A. H. (1999). Results of particle impact tests, *Impact Research Group Report IRG 13*. The Open University, Milton Keynes, UK.

Haff, P. K. (1983). Grain flow as a fluid-mechanical phenomena. *Journal of Fluid Mechanics*, *134*, 401–430.

Henein, H., Brimacombe, J. K., & Watkinson, A. P. (1983). Experimental study of transverse bed motion in rotary kilns. *Metallargical Transactions B*, *14*, 191–205.

Hill, H. M. (1966). Bed forms due to fluid stream. *Journal of the Hydraulic Division of the American Society of Civic Engineers*, *92*, 127–143.

Hoomans, B. P. B. (2000). *Granular dynamics of gas–solid two-phase flows*. Ph.D. thesis, University of Twente. Netherlands.

Hsiau, S. S., & Hunt, M. L. (1993). Kinetic theory analysis of flow-induced particle diffusion and thermal conduction in granular material flows. *Journal of Heat Transfer*, *115*, 541–548.

Hsiau, S. S., & Shieh, Y. M. (2000). Effect of solid fraction on fluctuations and self-diffusion of sheared granular flows. *Chemical Engineering Science*, *55*, 1969–1979.

Hunt, M. L. (1991). Comparison of convective heat transfer in packed beds and granular flows. In C. L. Tien (Ed.), *Annual review of heat transfer* Vol. 3 (pp. 163–193) New York: Hemisphere Publishing Corporation, (Chapter 6).

Johnson, P. C., & Jackson, R. (1987). Frictional-collisional constitutive relations for granular materials with application to plane shearing. *Journal of Fluid Mechanics*, *176*, 67–93.

Johnson, P. C., Nott, P., & Jackson, R. (1990). Frictional-collisional equations of motion for particulate flows and their application to chutes. *Journal of Fluid Mechanics*, *210*, 501–535.

Khakhar, D. V., McCarthy, J. J., Shinbrot, T., & Ottino, J. M. (1997). Transverse flow and mixing of granular materials in rotating cylinders. *Physics of Fluids*, *9*, 31–43.

Kline, S. J. (1965). *Similitude and approximation theory*. New York: McGraw-Hill.

Lan, Y., & Rosato, A. D. (1995). Macroscopic behaviour of vibrating beds of smooth inelastic spheres. *Physics of Fluids*, *7*, 1818–1831.

Lun, C. K. K., Savage, S. B., Jeffery, D. J., & Chepurniy, N. (1984). Kinetic theories for granular flow: inelastic particles in Couette flow and slightly inelastic particles in a general flowfield. *Journal of Fluid Mechanics*, *140*, 223–256.

Lun, C. K. K. (1991). Kinetic theory for granular flow of dense, slightly inelastic, slightly rough spheres. *Journal of Fluid Mechanics*, *233*, 539–559.

Maw, N., Barber, J. R., & Fawcett, J. N. (1981). The oblique impact of elastic spheres. *Wear*, *38*, 101–105.

Natarajan, V. V. R., & Hunt, M. L. (1997). Heat transfer in vertical granular flows. *Experimental Heat Transfer*, *10*, 89–107.

Nott, P., & Jackson, R. J. (1992). Frictional-collisional equations of motion for granular materials and their application to flow in aerated chutes. *Journal of Fluid Mechanics*, *241*, 125–144.

Parker, D. J., Broadbent, C. J., Fowles, P., Hawkesworth, M. R., & McNeil, P. (1993). Positron emission particle tracking—a technique for studying flow within engineering equipment. *Nuclear Instruments and Methods of Physical Research A*, *326*, 592–607.

Parker, D. J., Dijkstra, A. E., Martin, T. W., & Seville, J. P. K. (1997). Positron emission particle tracking studies of spherical particle motion in rotating drums. *Chemical Engineering Science*, *52*, 2011–2022.

Patton, J. S., Sabersky, R. H., & Brennen, C. E. (1986). Convective heat transfer to rapidly flowing, granular materials. *International Journal of Heat Mass Transfer*, *29*, 1263–1269.

Rutgers, R. (1965). Longitudinal mixing of granular material flowing through a rotating cylinder—Part I. Descriptive and theoretical. *Chemical Engineering Science*, *20*, 1079–1087.

Savage, S. B. (1984). The mechanics of granular flows. *Advances in Applied Mechanics*, *24*, 289–367.

Savage, S. B., & Hutter, K. (1989). The motion of a finite mass of granular material down a rough incline. *Journal of Fluid Mechanics*, *199*, 177–215.

Savage, S. B. (1998). Analyses of slow high-concentration flows of granular materials. *Journal of Fluid Mechanics*, *377*, 1–26.

Sondergaard, R., Chaney, K., & Brennen, C. E. (1990). Measurements of solid spheres bouncing off flat plates. *Journal of Applied Mechanics*, *57*, 694–700.

Spurling, R. J. (2000). Granular flow in an inclined rotating cylinder: steady state and transients. *Ph.D. thesis*, Department of Chemical Engineering, University of Cambridge.

Sullivan, W. N., & Sabersky, R. H. (1975). Heat transfer to flowing of granular media. *International Journal of Heat Mass Transfer*, *18*, 97–107.

Walton, O. R., & Braun, R. L. (1986). Stress calculations for assemblies of inelastic spheres in uniform shear. *Acta Mechanica*, *63*, 73–86.

Walton, O. R., & Braun, R. L. (1993). Simulation of rotary-drum and repose tests for frictional spheres and rigid sphere clusters, in *Proceedings of Joint DOE/NSP Workshop on Flow of Particulate and Fluids*, Ithaca, New York.

Wes, G. W. J., Drinkenburg, A. A. H., & Stemerding, S. (1976). Solids mixing and residence time distribution in a horizontal rotary drum reactor. *Powder Technology*, *13*, 177–184.

Yamane, K. (1997). Dynamics of granular flows. *Ph.D. thesis*, University of Osaka, Japan.

Zablotny, W. W. (1965). The movement of the charge in rotary kilns. *International Chemical Engineering*, *5*, 360–366.